#### Contents lists available at ScienceDirect

## Scripta Materialia

journal homepage: www.elsevier.com/locate/scriptamat



# Experimental observations of "reversible" transformation toughening

J. Makkar<sup>a,1</sup>, B. Young<sup>b,1</sup>, I. Karaman<sup>b</sup>, T. Baxevanis<sup>a,\*</sup>

- <sup>a</sup> Department of Mechanical Engineering, University of Houston, Houston, TX 77204-4006, USA
- <sup>b</sup> Department of Materials Science and Engineering, Texas A&M University, College Station, TX 77843, USA



#### ARTICLE INFO

Article history: Received 28 August 2020 Revised 10 September 2020 Accepted 11 September 2020 Available online 20 September 2020

Keywords: Fracture Toughness Martensitic phase transformation Shape memory alloys

#### ABSTRACT

Materials with the propensity to undergo irreversible deformation display an increasing resistance to progressive crack advance, *i.e.*, stable crack growth. A one-parameter description of stable crack growth by a fracture toughness vs. crack advance (resistance) curve is possible under specific conditions. Here, experimental observations are reported to (i) demonstrate that the toughness enhancement due to crack advance in hysteretic materials may be "reversed" by partial unloading, which has implications on the evaluation of the resistance curve and its validity conditions, and (ii) provide an experimental verification of the theoretical insight into the mechanics of stable crack growth.

© 2020 Acta Materialia Inc. Published by Elsevier Ltd. All rights reserved.

In most dissipative material systems, cracks initially grow stably under increasing load until critical conditions are met. Such material systems are characterized by rising crack extension resistance curves, the so-called *R*-curves [1]. The *R*-curve slope is indicative of the relative crack growth stability and, thus, the entire *R*-curve provides a more complete description of the fracture response than a single fracture toughness value.

A simplistic rationale to stable crack growth is offered by the "energetic" argument that in order to maintain crack growth, energy must be supplied into the system to compensate for the work expended into the dissipative processes that accompany crack advance. In conventional ductile materials, the consensus is that crack growth is stabilized by irreversibility effects associated with nonproportional straining in the active plastic zone and the irrecoverable deformation left in the wake of the growing crack [2-6]. It has been argued that (i) plastically deformed solids offer more resistance to nonproportional loading, which corresponds to advancing cracks, than to (nearly) proportional loading, which corresponds to stationary cracks, and, therefore, the strain at given distances from the crack tip are generally larger in stationary problems than in crack growth problems for the same crack configuration and load under small-scale yielding conditions; thus, it is necessary to continue to deform the material in order to maintain a suitably concentrated strain field at the advancing crack tip, and (ii) there is a fan ahead of the crack tip such that residual plastic deformation behind that fan and at sufficiently small distances from the crack tip impedes crack growth. The construction of the *R*-curve for such materials is based on concepts of elastic-plastic fracture mechanics, employing the *J*-integral as the fracture criterion [7]. The *J*-integral is based on nonlinear elasticity and inadequately models nonproportional inelastic deformation. However, under *J*-controlled crack growth conditions [8], which require nearly proportional inelastic deformation everywhere but in a small neighborhood of the crack tip, the *J*-integral can still be used to analyze crack growth.

Similar to ductile metals, phase transforming materials display stable crack growth under increasing load, known as transformation toughening [9–21]. In reversible phase transforming materials, reversibility of phase transformation and reorientation of martensite variants render the phenomenon of stable crack growth even more complicated than that in most ductile metals. These materials may fail by a combination of ductile tearing and cleavage, e.g., NiTi and other Shape Memory Alloys (SMAs) [22,23], and it is not yet clear what is the effect of reorientation on the singularity of the strain fields close to the crack tip or whether the reversibility of phase transformation promotes or impedes crack advance [24,25].

The present study offers the first experimental investigation of the effect of the reversibility of inelastic deformation on the apparent fracture toughness of advancing cracks and its implications in measuring resistance curves. NiTi compact tension specimen are tested under isothermal mechanical loading at a temperature at which phase transformation is reversible (superelastic loading). The loading paths include unloading to induce reverse phase transformation beyond that occurring during crack advance. The experimental observations in this study offer evidence that (i) partial unloading during stable crack growth may have a substantial

<sup>\*</sup> Corresponding author.

E-mail addresses: jmakkar1004@gmail.com (J. Makkar), bey1@tamu.edu (B. Young), ikaraman@tamu.edu (I. Karaman), tbaxevanis@uh.edu (T. Baxevanis).

<sup>&</sup>lt;sup>1</sup> These authors have contributed equally to this letter.

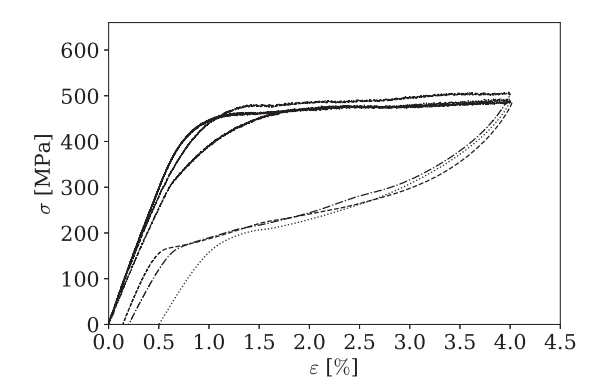


Fig. 1. Uniaxial tensile loading–unloading stress–strain curves for 3 experiments performed on  $Ni_{55.7}Ti$  (wt.%) at room temperature.

impact on the fracture response, (ii) the compliance method for constructing the *R*-curve should be used with caution, and (iii) the validity conditions of *R*-curves are more strict in hysteretic materials than in conventional structural metals and, thus, the *R*-curve as a means to study the stability of a real structure is even less effective.

A binary Ni<sub>55.7</sub>Ti<sub>44.3</sub> (wt.%) (Fig. 1), superelastic at room temperature, with phase transition temperatures  $M_f = -29$  °C,  $M_s =$  $-20 \,^{\circ}$ C,  $A_s = -15 \,^{\circ}$ C and  $A_f = 7 \,^{\circ}$ C, where  $M_f$ ,  $M_s$ ,  $A_s$  and  $A_f$  indicate martensite finish, martensite start, austenite start and austenite finish temperatures, respectively, was acquired from Fort Wayne Metals. The fracture tests are performed on compact tension specimens (schematic in Fig. 2a) at room temperature in an MTS-810 servo-hydraulic test frame. The dimensions of the specimen are W = 32.5, B = 8.5,  $0.45 \le a/W \le 0.55$ , all in mm. The specimens are fatigue pre-cracked in load control with load values between 0 and  $P_{\text{max}}$  at a frequency of 10 Hz, where  $P_{\text{max}}$ , initially set equal to 20% of the highest load value expected in the subsequent fracture experiment, and was gradually decreased. The precracked specimens are loaded in displacement control at a loading rate of 0.09 mm/min. Load and load line displacement using a clip on crack tip opening displacement extensometer by Epsilon Technology Corp are measured continuously at a rate of 10 Hz throughout the test. Optical images are recorded at a rate of 2 fps from one side of the CT specimens, which is speckled to produce a random pattern, using a Point Grey Blackfly CCD cameras equipped with Canon 18--55 mm lens at an optical resolution of 0.02 mm/pixel. The optical images are post-processed via Vic2D-6 software (developed by Correlated Solutions) to measure the full-field Lagrangian strain using Digital Image Correlation (DIC) [26].

Load-load line displacement curves from the superelastic NiTi CT specimens that are unloaded/reloaded once are presented in Fig. 2(a and b). In both cases, the material response is initially linear, followed by a nonlinearity associated with inelastic deformation: martensitic transformation, reorientation of martensite variants during crack advance, and possibly plastic deformation. During unloading back to 50% of the load, the behavior is again first linear followed by a nonlinear regime that is attributed to reverse phase transformation. Subsequent reloading displays a behavior similar to that of the initial loading with the load-load line displacement curves reaching eventually a peak value before descending to failure. A critical difference between the observed response and the respective one of conventional ductile metals and SMAs that do not display reverse phase transformation upon unloading (non-superelastic) (Fig. 4(c and d)) is the absence of a master curve, i.e., the load-displacement curve after the unloading/reloading cycle does not return to the point at which unloading took place. This response should be attributed to (i) the recovery of the phase transformation strains left in the wake of the growing crack that are not fully restored during reloading, and (ii) the different direction and magnitude of the martensite variants formed upon reloading in the active transformation zone.

DIC results depicting the surface strains close to the crack tip are presented in Fig. 3 at the instances denoted with a circle in Fig. 2b. Point ① corresponds to the instant of unloading and point 2 to the instant at which the crack starts growing again upon reloading. According to these results, there is marked difference on the strain field that results in crack advance once sufficient unloading has taken place. The straining corresponding to point @ in the load-load line displacement curve is in general lower than that corresponding to point ① at given distances from the crack tip and there is straining in the wake of the growing crack that is not fully recovered upon reloading. Moreover, the strain field is not as symmetric and smooth at point @ as is at point 10 (note the isocurve lines). As pointed out above, the aforementioned differences may also originate from the different direction and magnitude of the martensite variants formed upon reloading due to (i) changes in the loading direction in regions where reorientation took place during crack advance before unloading, (ii) cyclic effects in the transformation response, and (iii) local stress redistribution due plastic deformation.

The resulted drop in the J-value required for crack advance due to unloading, *i.e.*, the difference,  $J_1 - J_2$ , between the J-values at points  $\odot$  and  $\odot$ , is calculated using the methodology developed by Haghgouyan *et al.* [21] that relies on the ASTM E1820 [7] standard developed for conventional ductile materials. This methodology accounts for the change in the elastic properties induced by phase transformation, which, nevertheless, was shown to have a minor impact on the fracture toughness [27].  $J_1 - J_2$  is calculated from the load–load line displacement record by replacing the portion underneath the curve, area  $\bigcirc$  (Fig. 2d), with area  $\bigcirc$  in the following

equation, which approximates the J-value,

$$J = J^{el} + J^{in} = \frac{\eta^{el} A^{el}}{Bb} + \frac{\eta^{in} A^{in}}{Bb}. \tag{1}$$

 $A^{el}$  and  $A^{in}$  are the elastic and inelastic components of the area under the load–displacement curve, respectively, b=W-a is the length of the unbroken ligament, and  $\eta^{el}$  and  $\eta^{in}$  are geometry-dependent factors [21,27]. Namely,

$$J_{1} - J_{2} := -\left(J_{A}^{el} + J_{A}^{in}\right) + \left(J_{B}^{el} + J_{B}^{in}\right)$$

$$= -\left(\frac{\eta^{el}A_{A}^{el}}{Bb} + \frac{\eta^{in}A_{A}^{in}}{Bb}\right) + \left(\frac{\eta^{el}A_{B}^{el}}{Bb} + \frac{\eta^{in}A_{B}^{in}}{Bb}\right) \approx 7 \text{ KJ/m}^{2}, \quad (2)$$

where  $A_A^{el}$  and  $A_A^{in}$  determine the elastic and inelastic components of the energy released upon unloading (region (A)), respectively, and  $A_R^{el}$  and  $A_R^{in}$  determine the corresponding components of the energy stored upon reloading (region (B)) (Fig. 2d). The crack length needed for evaluating b is measured by the evolution of the elastic compliance [7,28]. The level of decrease of the "apparent" toughness value is roughly 8% of the  $J_1$ -value,  $J_1 \approx 88 \text{ KJ/m}^2$ ; in general, it is dependent on the extend of unloading, i.e., the extend of recovery of the phase transformation strains. It should be noted that the value  $J_1 \approx 88 \text{ KJ/m}^2$  is approximated by Eq. (1), which holds for static cracks. For advancing cracks, Eq. (1) should be corrected [7]. According to the ASTM standards, such a correction requires multiple unloading/reloading cycles. A similar analysis yields that the drop in the "apparent" fracture toughness due to the unloading-reloading cycle in the experiment of Fig. 2a is approximately 2 KJ/m<sup>2</sup>.

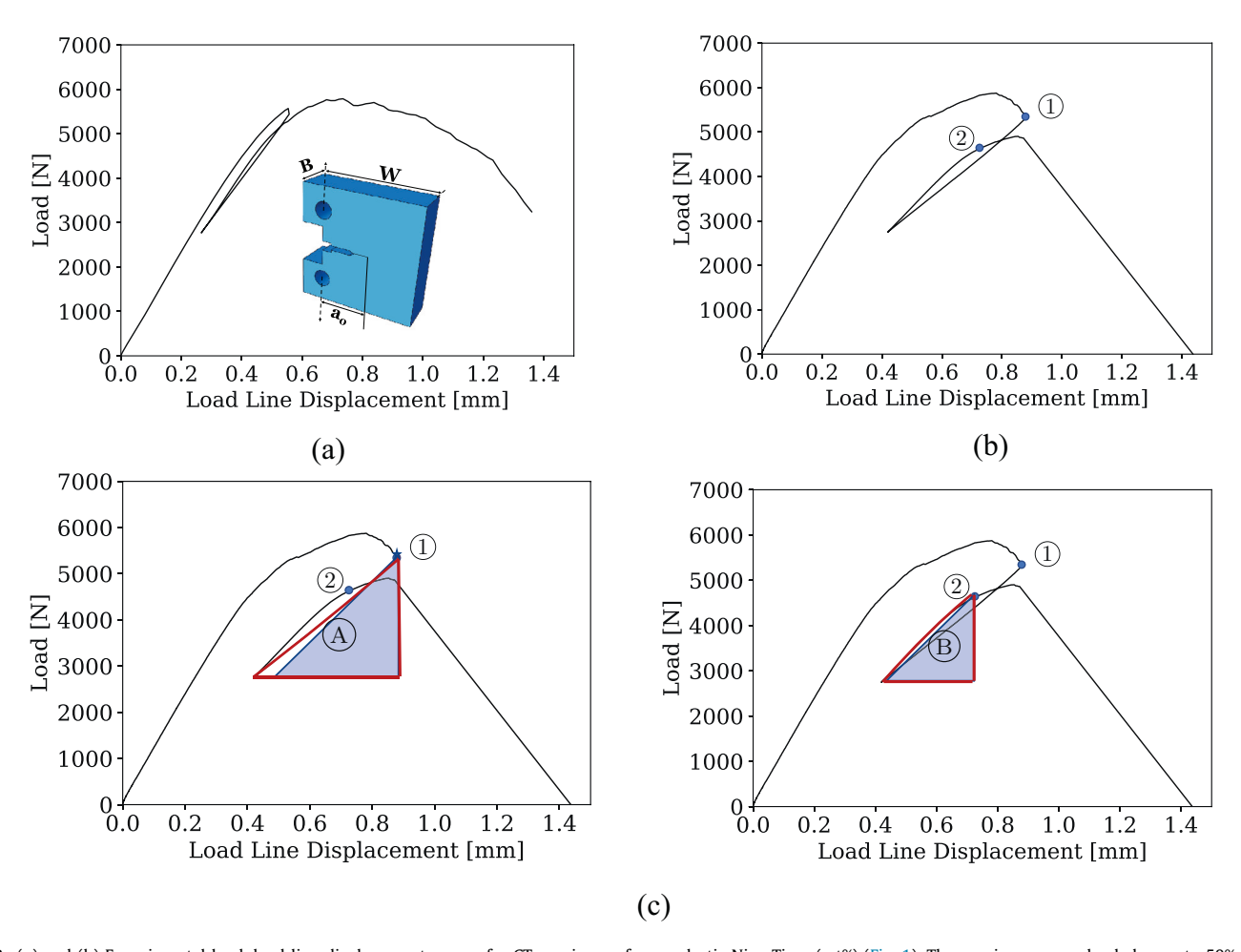


**Fig. 2.** (a) and (b) Experimental load-load line displacement curves for CT specimen of superelastic Ni<sub>55.7</sub>Ti<sub>44.3</sub> (wt%) (Fig. 1). The specimen are unloaded once to 50% of the load at the instant of unloading; (c) The regions  $\stackrel{\frown}{A}$  and  $\stackrel{\frown}{B}$  under the load-load line displacement are used for calculating the difference in the *J*-values between points  $\stackrel{\frown}{O}$  and  $\stackrel{\frown}{O}$ . Both regions are included within the solid (red) line.  $A_B^{el}$  and  $A_B^{el}$  are the shaded regions within  $\stackrel{\frown}{A}$  and  $\stackrel{\frown}{B}$ , respectively, and  $A_A^{in}$  and  $A_B^{in}$  are the remaining portions.

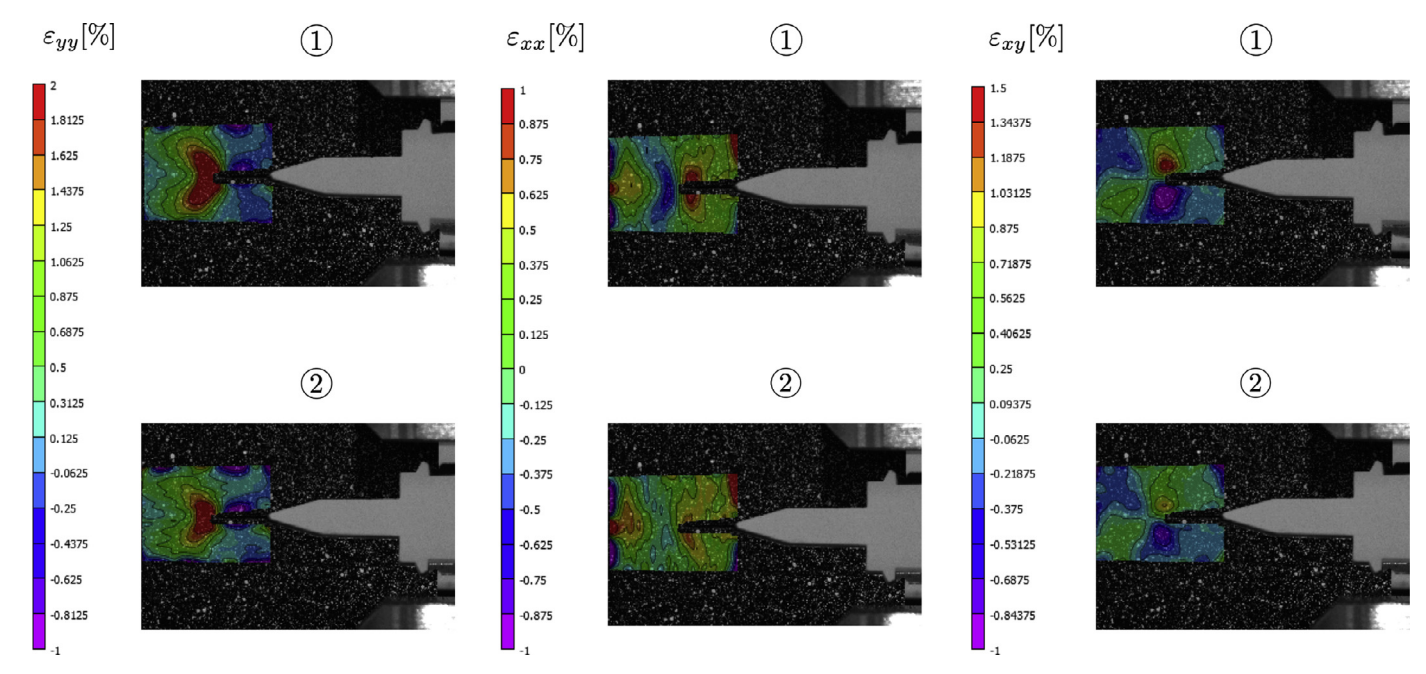
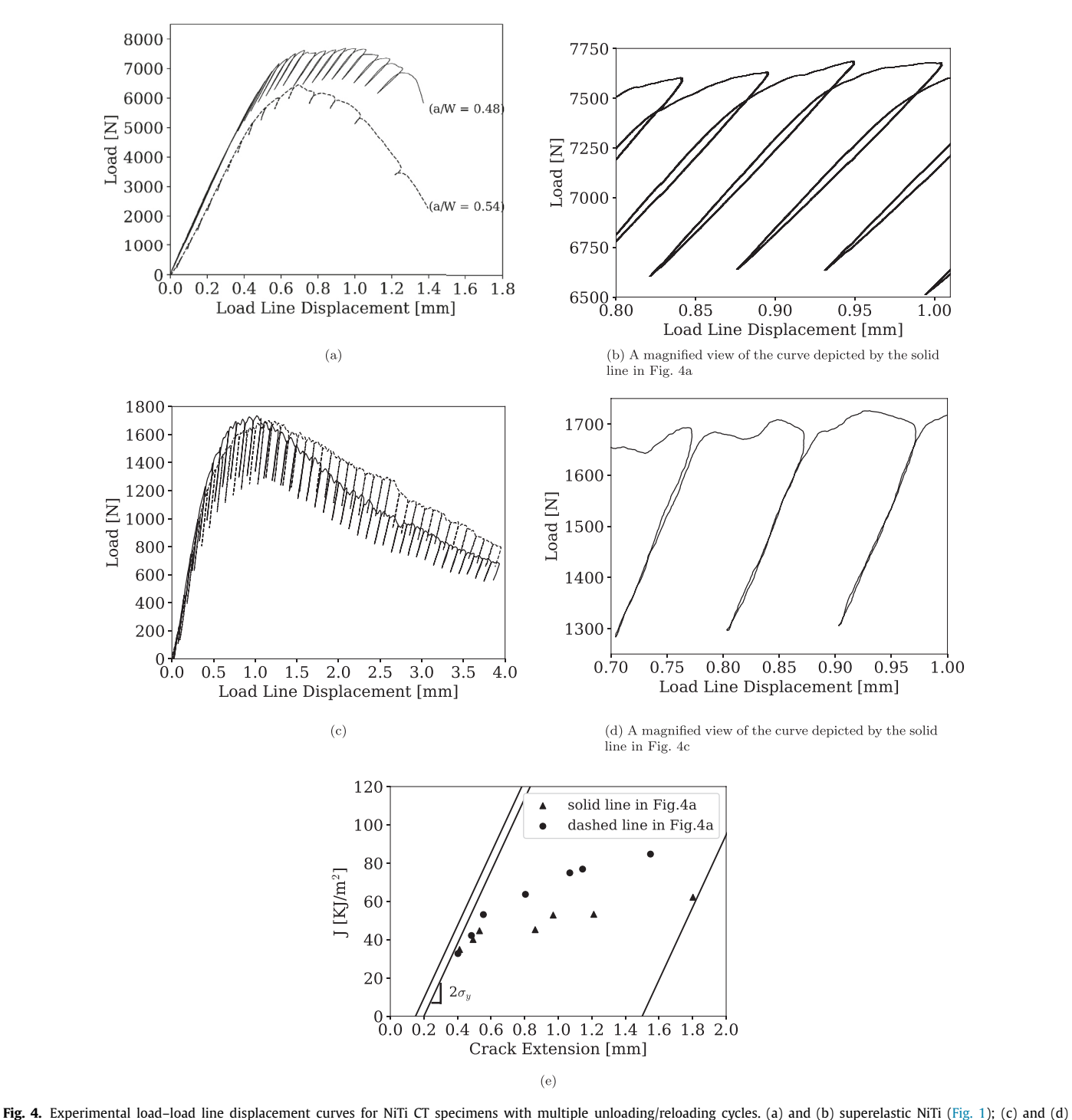


Fig. 3. Surface strain contour plots obtained from in situ DIC referring to points ① and ② in Fig. 2b. The y-axis is in the direction of loading.



Non-superelastic (solution heat-treated) NiTi [21]. The unloading is just a fraction of the maximum allowed in ASTM E1820 [7] standards, *i.e.*, 50% of the load at the instant of unloading. Note that the CT specimen width in (c) and (d) was just a fraction of the corresponding width in (a) and (b) ( ~ 3 mm vs 8.5 mm), which explains the marked difference on the load levels obtained on the respective experiments; (e) *R*-curves from the experiments on the superelastic NiTi (Fig. 4(a and b)). The solid lines in (e) represent the construction lines, *i.e.*, the exclusion lines and the 0.2 mm offset line, needed for the experimental measurement of the *R*-curve according to the ASTM standards [7].

Further experiments are performed with multiple unloading/reloading cycles as recommended by the ASTM standards for measuring *R*-curves. From the unloading/reloading cycles, the elastic compliance is measured, which is needed for distinguishing between the elastic and inelastic components in the ASTM recommended incremental correction of (1) for advancing cracks [7] (Fig. 4(a and b)). In these experiments, the unloading is smaller than 50% of the load at the instant of unloading, which

is the unloading performed in the experiments presented thus far and corresponds to the maximum value permitted in the ASTM standards. Moreover, for comparison purposes, load–load line displacement curves from experiments performed on solution heat-treated NiTi CT specimen are shown in Fig. 4(c and d). The material in these experiments is prone to plastic deformation and non-superelastic. A magnified view of the experimental curves shows that the material response of the superelastic NiTi during the

unloading/reloading cycle is still nonlinear (Fig. 4b) in contrast to the respective response of the non-superelstic NiTi (Fig. 4d) and the conventional ductile metals. The deviation from linearity is not as pronounced as it was in the experiments presented in Fig. 2 due to the smaller recovery of the transformation strains by the lower extend of unloading. Therefore, the resulted change in the J-value needed for crack advance due to an unloading/reloading cycle is not as drastic as that in the previous experiments. However, the cumulative effect of multiple unloading/reloading cycles may still have a substantial impact on both the load-load line displacement curve (Fig. 4a) and the resistance curve (Fig. 4e). Thus, the extent of unloading, which in one experiment (solid line) is triple that in the other (dashed line) should be responsible, together with material variability, for the pronounced discrepancy in the R-curves obtained from the two experiments (Fig. 4e) using the methodology detailed in Makkar and Baxevanis [27].

In conclusion, the presented experiments suggest that the driving force required for crack advance in superelastic SMAs can be altered through simple unloading, i.e., the transformation toughening associated with crack advance is reversible. This response is attributed to the impact of reverse phase transformation on the crack tip strain field in an unloading/reloading cycle and has implications on the evaluation and range of validity of the resistance curve. An R-curve measured according to the ASTM standards may no longer be treated as a "material property" since it may substantially differ from an R-curve response under monotonic loading. Thus, the ability of an R-curve obtained according to the standards to describe effectively resistance against stable growth and tearing instability is rather constrained, which limits its applicability in practical engineering, e.g., fitness-for-service evaluation or structural integrity assessment for engineering components and structures.

### **Declaration of Competing Interest**

Authors declare that they have no conflict of interest.

#### Acknowledgments

This study was supported by the US Air Force Office of Scientific Research under grant no. FA9550-15-1-0287, the National Science Foundation under grants no. CMMI-1917441 and CMMI-1917367, and by NASA-ULI under grant no. NNX17AJ96A.

#### References

- [1] X. Zhu, J. Joyce, Eng. Fract. Mech. 85 (2012) 1.
- [2] J. Hutchinson, On Steady Quasi-Static Crack Growth, 1974, Technical Report DEAP S-8, Division of Applied Sciences, Harvard University.
- [3] J.R. Rice, Mechanics and mechanisms of crack growth (proc. 1973), 1975, 14-
- [4] W. Drugan, J. Rice, T.L. Sham, J. Mech. Phys. Solids 30 (1982) 447.
- [5] J.R. Rice, R.M. McMeeking, D.M. Parks, E. Sorensen, Comput. Methods Appl. Mech. Eng. 411 (1979) 17–18.
- [6] R. Dean, J. Hutchinson, Fracture mechanics, ASTM-STP 700, 1980, 383-405.
- [7] ASTM-E1820, Standard Test Method for Measurement of Fracture Toughness, 2016, Technical report, ASTM International, West Conshohocken, PA.
- [8] J. Hutchinson, P. Paris, in: ASTM International, 1979, pp. 37–64.
- [9] R. Pohanka, S. Freiman, B. Bender, J. Am. Ceram. Soc. 61 (1978) 72.
- [10] F. Lange, J. Mater. Sci. 17 (1982) 235.
- [11] R. McMeeking, A. Evans, J. Am. Ceram. Soc. 65 (1982) 242.
- [12] B. Budiansky, J. Hutchinson, J. Lambropoulos, Int. J. Solids Struct. 19 (1983) 337.
- [13] A. Evans, R. Cannon, Acta Metall. 34 (1986) 761.
- [14] D.B. Marshall, J. Am. Ceram. Soc. 69 (1986) 173.
- [15] K. Mehta, A. Virkar, J. Am. Ceram. Soc. 73 (1990) 567.
- [16] C. Landis, J. Mech. Phys. Solids 51 (2003) 1347.
- [17] S. Robertson, R. Ritchie, Biomaterials 28 (2007) 700.
- [18] J.R. Kelly, I. Denry, Dental Mater. 24 (2008) 289.
- [19] G. Lacroix, T. Pardoen, P. Jacques, Acta Mater. 56 (2008) 3900.
- [20] S. Gollerthan, M. Young, A. Baruj, J. Frenzel, W. Schmahl, G. Eggeler, Acta Mater. 57 (2009) 1015.
- [21] B. Haghgouyan, C. Hayrettin, T. Baxevanis, I. Karaman, D. Lagoudas, Acta Mater. 162 (2019) 226.
- [22] K. Gall, N. Yang, H. Sehitoglu, Y. Chumlyakov, Int. J. Fract. 109 (2001) 189.
- [23] J. Olsen, Z. Zhang, H. Lu, E.C. van der, Eng. Fract. Mech. 84 (2012) 1.
- [24] G. Stam, G.E. van der, Mech. Mater. 21 (1995) 51.
- [25] T. Baxevanis, C.M. Landis, D.C. Lagoudas, J. Appl. Mech. 81 (2014) 041005.
- [26] H. Schreier, J.J. Orteu, M.A. Sutton, Image Correlation for Shape, Motion and Deformation Measurements, Springer, US, 2009.
- [27] J. Makkar, T. Baxevanis, J. Intell. Mater. Syst. Struct. 31 (2020) 475.
- [28] J. Joyce, J. Gudas, in: ASTM International, 1979, pp. 451-468.